Advances in Science and Technology Research Journal

Advances in Science and Technology Research Journal, 2026, 20(5), 335–344
https://doi.org/10.12913/22998624/215671
ISSN 2299-8624, License CC-BY 4.0

Received: 2025.11.06
Accepted: 2026.03.15
Published: 2026.04.01

Determination of critical values of damage functions defining the initiation of crack propagation for cold-formed S355 steel

Patrycja Walczuk-Gągała[1*], Łukasz Wójcik[1], Zbigniew Pater[1]

[1] Lublin University of Technology, Nadbystrzycka 36, 20-618 Lublin, Poland
* Corresponding author's e-mail: p.walczuk@pollub.pl

ABSTRACT

The presented article focused on the issue of cracking in forgings obtained through metal forming processes. In metallic materials, ductile and brittle cracking can be distinguished. Due to the nature of the article, attention was focused on the criteria for ductile fracture. Experimental tests and numerical analyses have enabled the definition of damage function values for cylindrical specimens made of S355 steel in a rotational compression test within a channel under cold forming conditions, in accordance with nine currently used plastic fracture criteria. The paper also implemented the determination of the damage function value based on the Pater hybrid criterion. Numerical analyses were conducted in the Simufact. Forming v.15 software. During the tests, the distribution of stresses and strains was analysed, which enabled for the determination of stress triaxiality and critical values of the damage function for all examined ductile fracture criteria. The tests showed that the hybrid Pater fracture criterion and the other criteria analysed accurately predict the location of the fracture in the tested specimens in the rotational compression test conducted under cold working conditions.

Keywords: material fracture, ductile fracture criterion, rotational compression.

INTRODUCTION

Modern technologies that enable the plastic processing of metals allow for the formation of products in various forms, including pre-forgings and axisymmetric forgings. For shaping, among other methods, machines and devices that represent innovative solutions in the forging industry are used. A popular forming method is cross-wedge rolling, which unfortunately also has limitations, including uncontrolled slipping, necking, and tearing of the forged piece being shaped, as well as internal cracks in the formed product, resulting from the Mannesmann effect that occurs during the forming process [1]. These cracks are caused, among other things, by the occurrence of cyclic stresses and deformations in the central areas of the specimens or the gradual destruction of the material cohesion caused by low-cycle fatigue [2,3]. The research conducted by Pater showed that in the rotary compression test, the stress state is closest to the stress state present during cross-rolling and skew rolling [4–6]. Figure 1 shows two types of fracture in metallic materials – ductile and brittle [7].

In the case of ductile fracture, the crack arises as a consequence of the creation, growth and coalescence of voids [8]. This fracture is therefore characterised by a low growth rate after considerable plastic deformation. The fracture surface is rough and dull, and in a tensile test, the deformed specimen takes on a cup-and-cone shape. Brittle fracture is characterised by the breaking of atomic bonds along specific crystallographic planes [9]. The crack propagates rapidly, and the fracture surface is smooth and bright.

Models based on various fracture criteria are used to predict ductile fracture in plastically deformed materials [10]. The criteria are primarily intended to identify the location of the fracture and determine the critical damage value. In general, the function describing the damage of the material microstructure can be expressed as:

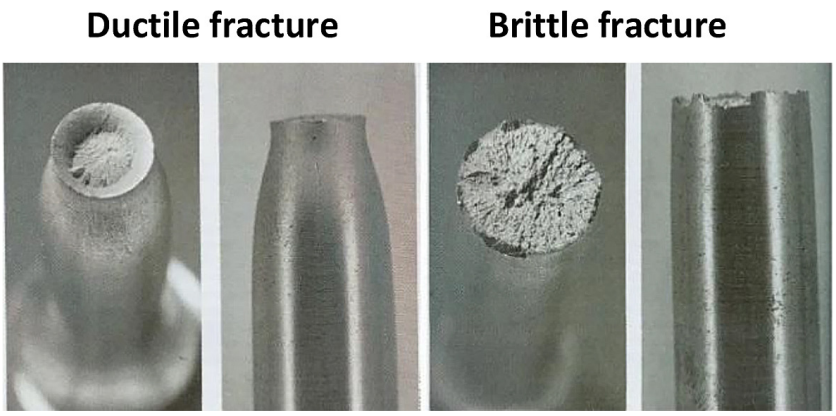

Figure 1. Classification of fracture morphology [9]

$$C = \int_0^{\varepsilon_f} \Phi(\sigma) d\varepsilon \tag{1}$$

where: C – the critical value of the damage function, ε_f – critical plastic strain at fracture, $\Phi(\sigma)$ – function describing the effect of stress on the rate of void formation and coalescence.

The literature allows identifying a set of ductile fracture criteria based on the function Φ(σ) (Table 1).

In a broad sense, the moment of damage is expected when the damage variable reaches a ratio equal to 1 in relation to C_{gr}:

$$\frac{C}{C_{gr}} \geq 1 \tag{2}$$

where: C_{gr} – the limit value of the damage function at the moment of fracture initiation.

Pater's hybrid criterion combines the basis of the ductile fracture criterion with the maximum shear stress criterion. Pater chose the most commonly used normalised Cockcroft-Latham criterion as the plasticity fracture criterion, referring to pure shear stress and utilising the Huber-Mises hypothesis [20]. The hybrid fracture criterion was expressed by the equation:

$$C_{PATER} = \int_0^{\varepsilon} \left[\begin{array}{c} (1-\Phi)\dfrac{\sqrt{3}}{2}\dfrac{\sigma_1 - \sigma_3}{\sigma_i} \\ +\Phi\dfrac{\sigma_1}{\sigma_i} \end{array} \right] d\varepsilon \tag{3}$$

$$\left\{ \begin{array}{c} \Phi = 0 \; for \; \eta \leq 0 \\ \Phi = 3 \; for \; 0 < \eta < 0.333 \\ \Phi = 1 \; for \; \eta \geq 0.333 \end{array} \right\}$$

where: C_{PATER} – damage function value according to Pater criterion, σ_1 – maximum principal stress, σ_3 – minimum principal stress, σ_i – effective stress, η – stress triaxiality, Φ – coefficient describing the fraction of ductile fracture in the damage function.

The aim of this article was to determine the critical values according to stress and dimensionless damage functions, as well as using the hybrid Pater criterion, employing S355 steel under cold working conditions.

MATERIAL AND METHODS

The text reviewed the results of research conducted on fracture criteria, along with a hybrid hypothesis of the Pater criterion for S355 steel, which is used in applications characterised by increased strength, dimensional accuracy and surface quality, e.g. in cold-formed profiles, bars, wires and structural sheets. The steel used for testing is non-alloy steel with the chemical composition reported in Table 2.

In order to determine the value of the damage function according to fracture criteria, laboratory tests and numerical simulations of rotational compression of specimens in a channel were carried out. The laboratory technique used allows the determination of the fracture moment resulting from the Mannesmann effect during the forming process in the channel. Cylindrical specimens with initial dimensions of 40 mm in diameter and 20 mm in length were used for the tests, which were placed in the channel of the lower tool. The specimens were rolled in a die with a height of 2 = 38.4 mm. The upper tool moved at a speed of v = 300 mm/s, while the lower remained stationary.

Table 1. Damage functions used in ductile fracture analysis

Criterion	Formula
Freudenthal [11]	$\int_0^{\varepsilon_f(t)} \sigma_i \, d\varepsilon \geq C_{FREU}$
Cockroft – Latham [12]	$\int_0^{\varepsilon_f(t)} \sigma_1 d\varepsilon \geq C_{CL}$
Oh [13]	$\int_0^{\varepsilon_f(t)} \frac{\sigma_1}{\sigma_m} d\varepsilon \geq C_{OH}$
Brozzo et al. [14]	$\int_0^{\varepsilon_f(t)} \frac{2\sigma_1}{3(\sigma_1 - \sigma_m)} d\varepsilon \geq C_{BROZ}$
Ayada [15]	$\int_0^{\varepsilon_f(t)} \frac{\sigma_m}{\sigma_i} d\varepsilon \geq C_{AYAD}$
Oyane [16]	$\int_0^{\varepsilon_f(t)} \left(1 + \frac{1}{A}\frac{\sigma_m}{\sigma_i}\right) d\varepsilon \geq C_{OYAN}$
Zhan et al. [17]	$\int_0^{\varepsilon_f(t)} (\sigma_1 - \sigma_m) d\varepsilon \geq C_{ZHAN}$
Rice & Tracey [18]	$\int_0^{\varepsilon_f(t)} exp\left(\frac{3}{2}\frac{\sigma_m}{\sigma_i}\right) d\varepsilon \geq C_{RT}$
Argon et al. [19]	$\int_0^{\varepsilon_f(t)} (\sigma_m + \sigma_1) d\varepsilon \geq C_{ARGO}$

Note: σ_1 – maximum principal stress, σ_m –mean stress, σ_i – effective stress.

Table 2. Chemical composition of S355 steel (weight percentage, %)

C	Mn	Si	P	S	Cr	Ni	Al	Cu	Fe
0.2	1.5	0.2–0.5	≤ 0.04	≤ 0.04	≤ 0.3	≤ 0.3	≤ 0.02	≤ 0.03	others

During forming, the specimen undergoes intense ovalisation of the cross-section, and the removal of this effect results in the elongation of the specimen. The walls of the channel counteract this, resulting in a variable state of compressive-tensile stresses along the entire length of the distance s in the axial zone of the specimen, which leads to the formation of a fracture known as the Mannesmann effect. In order to determine the critical forming distance for S355 steel, three specimens were allocated for each distance tested. Figure 2 shows a diagram of rotary compression.

For the experimental studies, a flat-wedge rolling mill (Figure 3a) was used, equipped with tools in the form of flat tools with a channel (Figure 3b), located at the Department of Metal Forming at Lublin University of Technology. The rolling mill allows specimens to be shaped using flat tools with a length not exceeding 1000 mm.

During the rotational compression tests in the channel, various values of the forming distance s were used to determine its critical value. Exceeding the critical value of the forming distance s caused a crack to form in the axial part of the specimen. Under these conditions, the distance s was decreased and the test was continued until a crack appeared on the side surface of the specimen. The test was then repeated with these parameters two more times, and if no cracking was observed, this value of the distance was considered critical for the material in question. Experimental tests were conducted at 20 °C. The flowchart describing the method of determining the critical damage function based on the new rotary compression test is given in Figure 4.

RESULTS

During experimental research, the critical deformation distance *s* was determined to be *s* = 500 mm. An increase in the deformation distance s results in

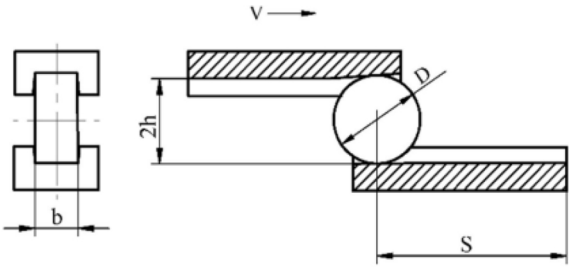

Figure 2. Scheme of rotary compression – specimens in the channel

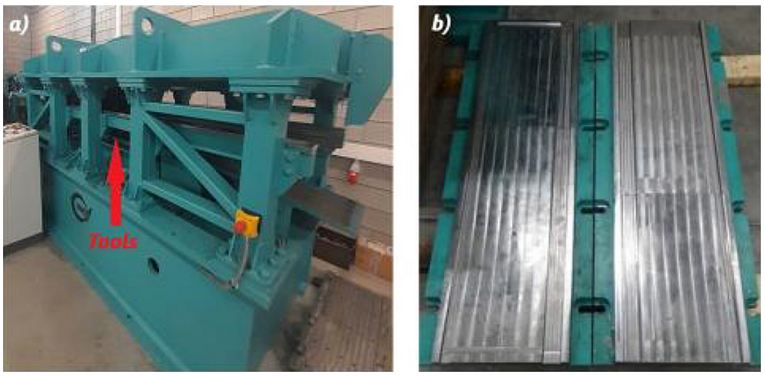

Figure 3. Laboratory setup: a) cross and wedge rolling mill, b) tools

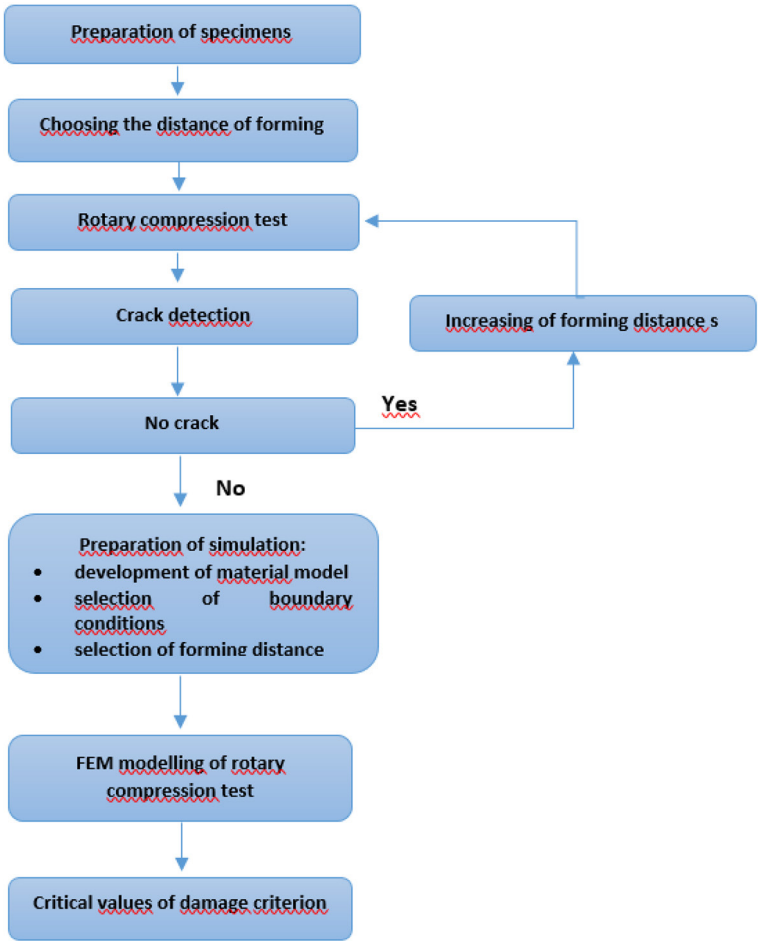

Figure 4. Flowchart describing the method of determining the critical damage function

an enlargement of the crack size in the radial direction. Figures 5–6 show the specimens deformed in the channel. After determining the critical value of the forming distance s, numerical modelling of the rotational compression test in the channel was undertaken using Simufact.Forming v.15 software. The geometric model created was identical to the one used in the laboratory test (Figure 7). Forming was performed on the critical distance *s*.

During numerical calculations, it was established that the speed of the upper tool movement was 300 mm/s. The material model was obtained from own plastometric tests and described by the following equation:

$$\sigma_F = 610.285 \cdot \varepsilon^{0.09} \tag{4}$$

where: σ_F – flow stress.

Figure 5. Deformed specimens achieved with a forming distance (s) equal to (from left to right) 500 mm, 600 mm and 800 mm

Figure 6. Cross-sections of deformed specimens achieved with a forming distance (s) equal to (from left to right) 500 mm, 600 mm and 800 mm

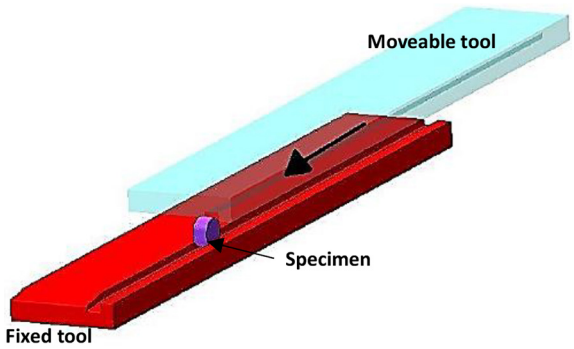

Figure 7. Model of the performed test created in Simufact.Forming

A friction factor of m=0.9 was established between the shaped material and the tools, while the temperature of the tools and specimens was kept constant at 20 °C. The heat transfer coefficient between the tool and the specimen was 20 000 W/m²·K. Hexahedral elements with a size of 1.5 mm were used for modelling. In order to quantitatively assess the issue under study, 21 sensors were installed on the specimen axis at 1 mm intervals to record the parameters needed to determine the damage function (Figure 8).

The numerical analysis conducted allowed for the determination of the distribution of effective strain (Figure 9) and the distribution of the damage function calculated based on the normalised Cockcroft-Latham criterion (Figure 10) along the critical distance $s = 500$ mm. The largest deformations occur on the side surfaces, where the material comes into contact with the side planes of the cut, while in the axial zone, the deformations are uniform. The damage distribution confirms the belief that the greatest material fracture in the rotational compression test in the channel will occur in the axial zone of the specimen – the function takes extreme values there, which are highest at the centre of the specimen and decrease as one approaches its front surfaces.

During experimental tests and numerical analysis, the values of the forming forces were recorded (Figure 11). The nature of the forces recorded during the experiment and numerical simulation is similar. During the initial stage of the process, the forming forces are most intense when the specimen undergoes significant ovalisation. In the next phase, the forces gradually decrease and remain relatively stable until the end of the rotational compression process.

The data collected from the sensors enabled determining the distribution of damage functions along the axis of the specimens. The distributions were grouped according to the nature of the damage function (stress functions – Figure 12 and dimensionless function – Figure 13). In the case of calculating the critical value according to Oyane's criterion, it was assumed that the material constant is equal to A = 0.424 [21]. Some of the calculated functions show similar behaviour, namely, the values of the damage function reach a peak at the centre of the specimen and decrease with distance from the centre. The criteria of Freudenthal, Zhan, Oyane, and Oh show a linear distribution along the entire length of the specimen. This indicates that these criteria determine that the probability of fracture is the same along the entire axis and has the same value in each sensor. The other criteria show that the damage function reaches its peak values in the middle of the specimens and then decreases towards the side surfaces.

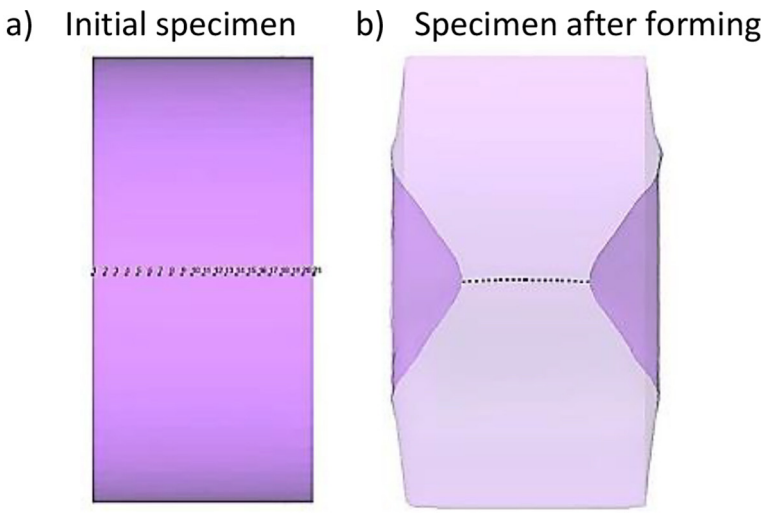

Figure 8. The arrangement of sensors along the specimens used to monitor parameters reporting the state of stress and strain: a) initial specimen, b) specimen after forming

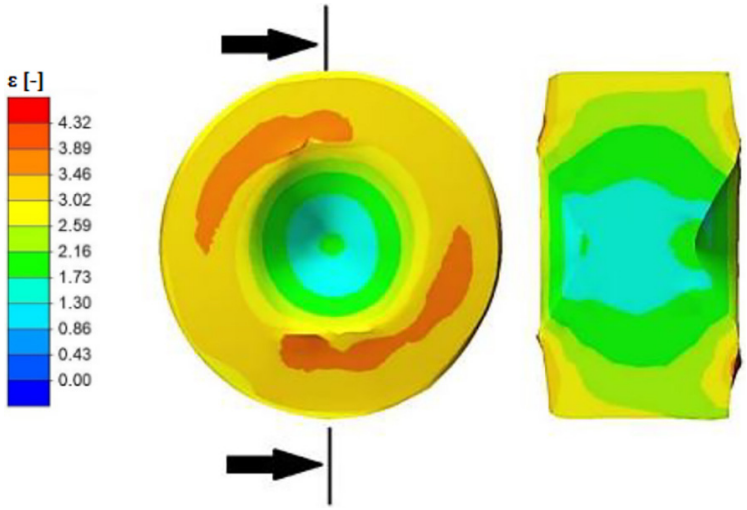

Figure 9. Distribution of effective strain in a specimen submitted to rotational compression

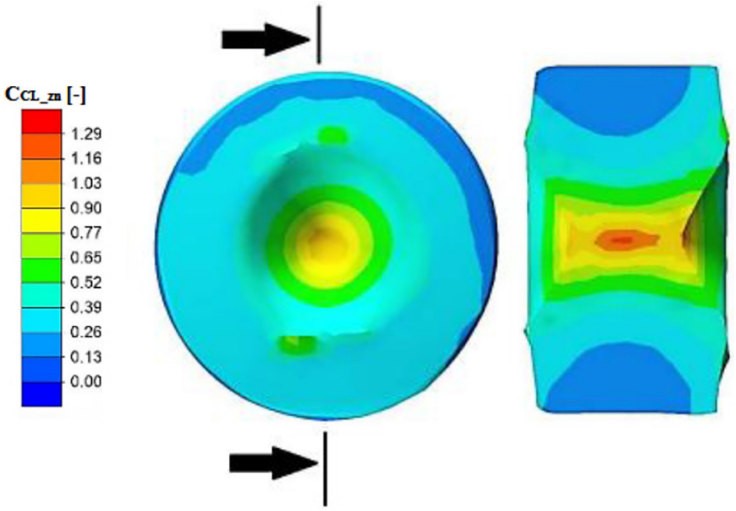

Figure 10. Distribution of the Cockroft-Latham damage function in a specimen submitted to rotational compression

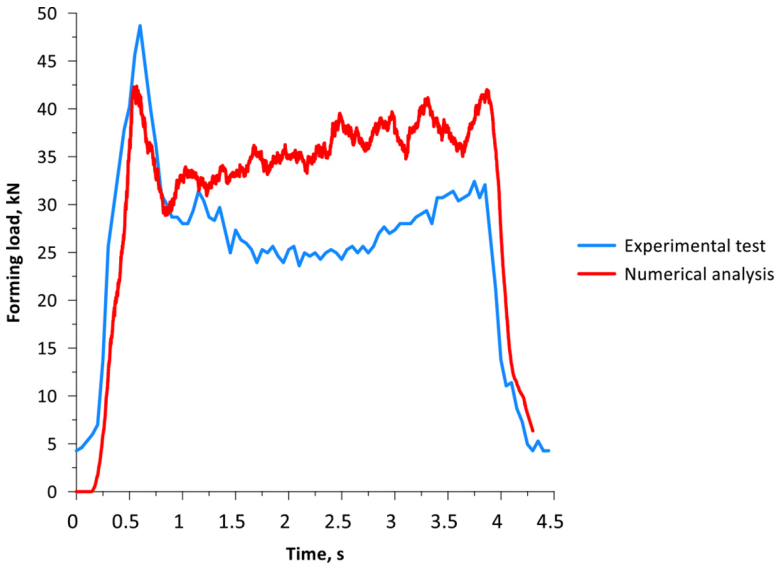

Figure 11. Comparison of forming loads distribution results obtained from experiments and numerical simulations for S355 steel with a forming distance of s = 500 mm

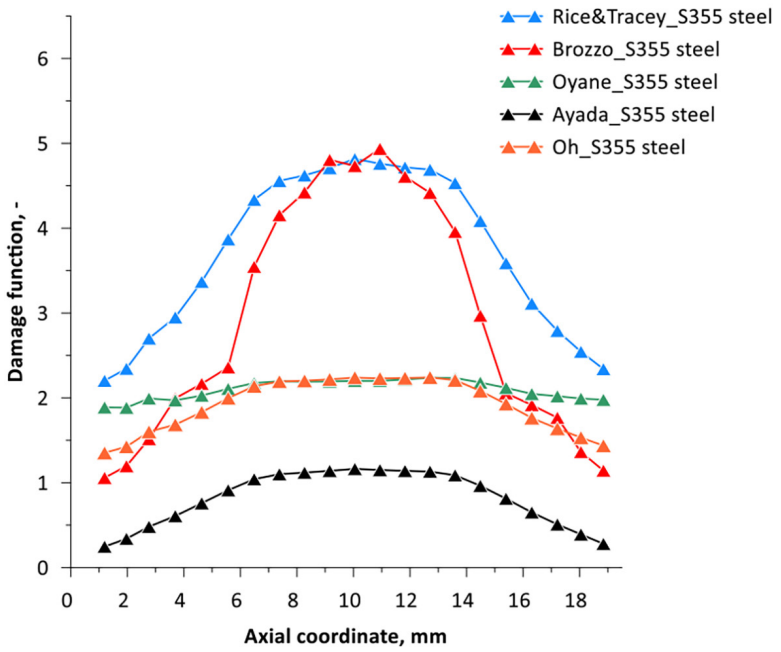

Figure 12. Distribution of the dimensionless functions for S355 steel in the rotary compression test, the specimen formed at the distance s = 500 mm

The placement of sensors in the test specimen enabled the determination of the stress triaxiality distribution. From the instantaneous values obtained in the specimen at a given sensor, the average values of the parameter were calculated (Figure 14), using the following relationship:

$$\eta_{śr} = \frac{1}{\varepsilon}\int_0^{\varepsilon} \eta d\varepsilon \tag{5}$$

where: ε – effective strain.

The measured values depend on the placement of the sensor. The stress triaxiality is higher at the centre of the specimen and reaches the lowest values at the side surfaces. On the basis of the results of computer simulations, the damage function value was computed by the Pater criterion based on a hybrid approach. The calculation results are illustrated in Figure 15 showing how the criterion value changes depending on the sensor position on the specimen axis.

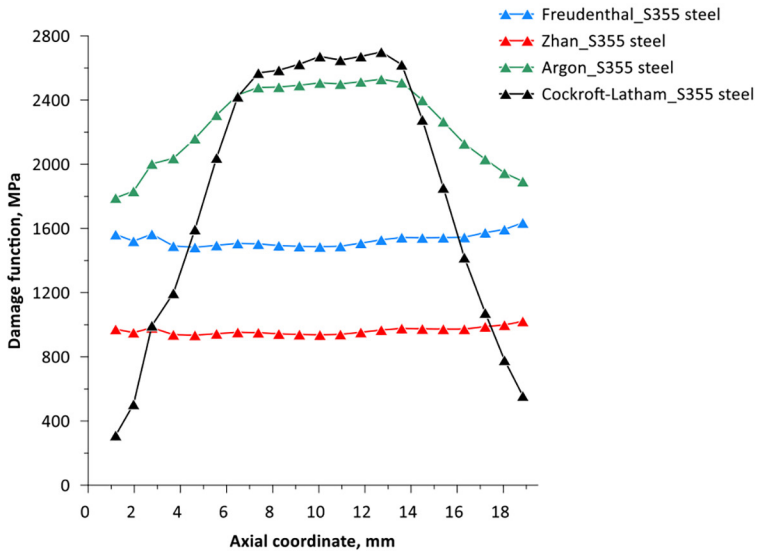

Figure 13. Distribution of stress functions for S355 steel in the rotary compression test, the specimen formed at the distance s = 500 mm

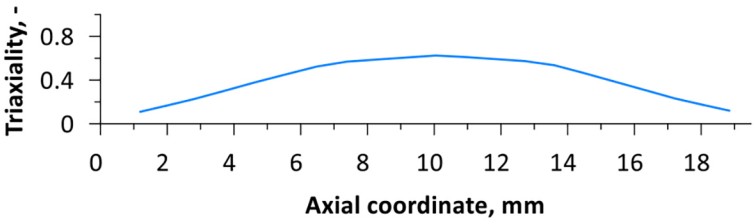

Figure 14. Distribution of stress triaxiality in the specimen axis

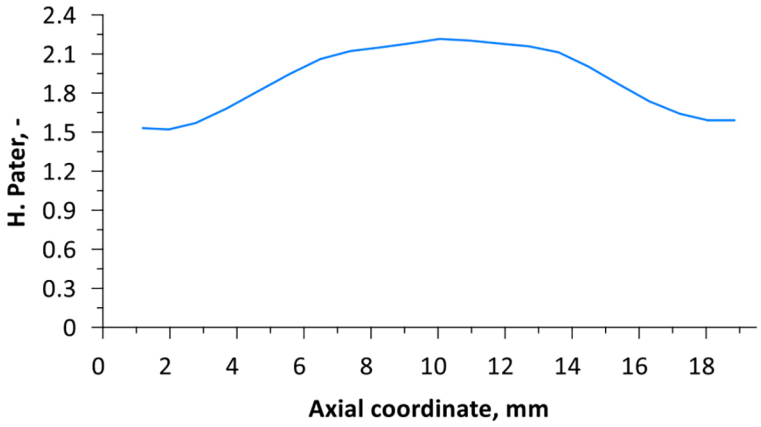

Figure 15. Change in the hybrid damage criterion by Pater at points situated along the specimen axis

Table 3. Critical values of the damage function for S355 steel in rotary compression test, in the temperature of 20 °C

Parameter	C_{FREU} [MPa]	C_{ZHAN} [MPa]	C_{ARGO} [MPa]	C_{CL} [MPa]	C_{RT}	C_{BROZ}	C_{OYAN}	C_{AYAD}	C_{OH}	C_{PATER}
Rotary compression	1528.7	962.5	2249.7	1683.5	3.7	2.91	2.1	0.81	1.91	2.21

Note: C_{ARGO} damage function value according to Argon's criterion, C_{AYAD} damage function value according to Ayada's criterion, C_{BROZ} damage function value according to Brozzo's criterion, C_{CL} damage function value according to Cockroft-Latham criterion, C_{FREU} damage function value according to Freudenthal's criterion, C_{OH} damage function value according to Oh's criterion, C_{OYAN} damage function value according to Oyane's criterion.

The values of the damage function presented in Table 3 are derived from the measurements taken. The average values from all sensors were taken as the critical values of the damage function.

CONCLUSIONS

The article presents the methodology, results of laboratory tests, and numerical simulations for the rotary compression test of S355 steel for a process conducted at 20 °C. These data enabled the determination of critical values of the damage function in the context of the adopted ductile fracture criteria. On the basis of the findings of the research, the following conclusions were drawn:

- Laboratory tests conducted allowed for the numerical verification of the rotary compression test in the channel,
- The values of dimensionless damage functions are in units, while the values of stress damage functions are in thousands,
- The values obtained from dimensionless and stress damage functions are not equal, but some of them accurately predict the location of the fracture – in the middle of the specimen,
- The Freudenthal, Zhan, Oyane, and Oh criteria show a linear distribution along the entire length of the specimen – according to them, the probability of fracture is the same along the entire axis and has the same value in each sensor,
- The value of the damage function according to the Ayada criterion is below 1 and is practically 4.5 times smaller than the value obtained from the Rice&Tracey criterion, while the value of the damage function according to the Zhan criterion is more than twice smaller than the value obtained from the Argon criterion,
- The value of the damage function obtained from the Freudenthal criterion is similar to the value from the Cockroft-Latham criterion, and the similarity in values can also be seen in the Pater and Oyane criteria.
- The hybrid fracture criterion accurately defines the location of crack occurrence in the case of S355 steel under cold processing conditions, i.e., at a temperature of 20 °C,
- Pater's hybrid fracture criterion can be used to predict fracture during processes occurring at ambient temperature, i.e. under cold conditions.

Acknowledgments

The research was funded by the Lublin University of Technology program titled "Investing in Potential" (Grant No:3/IP/2025/F).

REFERENCES

1. Pater Z., Weroński W., Podstawy teoretyczne procesu walcowania poprzeczno-klinowego, Lublin, Lubelskie Towarzystwo Naukowe, 1995.
2. Hashmi M.S.J., Comprehensive Materials Processing. 13 Volume Set, Amsterdam, Elsevier, 2014.
3. Pater Z., Weroński W., Gontarz A., Wybrane zagadnienia z teorii i technologii walcowania poprzeczno-klinowego, Lublin, Lubelskie Towarzystwo Naukowe, 2001.
4. Pater Z., Tomczak J., Bulzak T., Wójcik Ł., Lis K., Rotary compression in tool cavity–a new ductile fracture calibration test, The International Journal of Advanced Manufacturing Technology, 2020; 106(9–10): 4437–4449.
5. Pater Z., Tomczak J., Bulzak T., Wójcik Ł., Walczuk P., Assessment of ductile fracture criteria with respect to their application in the modeling of cross wedge rolling, Journal of Materials Processing Technology, 2020; 278: 1–11.
6. Pater Z., Tomczak J., Bulzak T., Wójcik Ł., Walczuk P., Determination of the critical value of damage in a channel-die rotational compression test, International Journal of Material Forming, 2020; 13(6): 993–1002.
7. Argon A.S., Im J., Safoglu R., Cavity formation from inclusions in ductile fracture, Metallurgical Transactions A, 1975; 6(4): 825–837.
8. Wei J., Yang L., Guo J., The method to determine material constants in ductile fracture criterion, Solid State Phenomena, 2018; 279: 85–91.
9. Callister W.D., Fundamentals of Materials Science and Engineering, USA, John Wiley&Sons, 2001.
10. Linardon C., Precision tube drawing for biomedical applications: theoretical, numerical and experimental study, praca doktorska, Université de Grenoble, 2013.
11. Freundenthal A.M., The inelastic behaviour of engineering materials and structures, New York, John Wiley & Sons, 1950.
12. Cockcroft M.G., Latham D.J., Ductility and workability of metals, Journal of the Institute of Metals, 1968; 96: 33–39.
13. Mirghasemi S.M., Eivani A.R., Seyedein S.H., Jafarian H.R., A comparison between routine vs. normalized Cockroft–Latham fracture criteria for prediction of fracture during equal channel angular pressing, Engineering Fracture Mechanics, 2018; 199: 721–729.

14. Brozzo P., DeLuca B., Rendina R., A new method for the prediction of formability in metal sheets, In: Proceedings of the 7th Biennial Conference of IDDRG on Sheet Metal Forming and Formability, 1972.
15. Ayada M., Higashino T., Mori K., Central bursting in extrusion of inhomogeneous materials. In: Proceedings of the First International Conference on Technology of Plasticity, 1984; 1: 553–558.
16. Oyane M., Sato T., Okimoto K., Shima S., Criteria for ductile fracture and their applications, Journal of Mechanical Working Technology, 1980; 4(1): 65–81.
17. Zhan M., Gu Ch., JIang Z., Hu L., Yang H., Application of ductile fracture criteria in spin-forming and tube-bending processes, Computational Materials Science, 2009; 47(2): 353–365.
18. Rice J.R., Tracey D.M., On the ductile enlargement of voids in triaxial stress fields, Journal of the Mechanics and Physics of Solids, 1969; 17(3): 201–217.
19. Argon A.S., Im J., Safoglu R., Cavity formation from inclusions in ductile fracture, Metallurgical Transactions A, 1975; 6(4): 825–837.
20. Pater Z., Tomczak J., Bulzak T., Establishment of a new hybrid fracture criterion for cross wedge rolling, International Journal of Mechanical Sciences, 2020; 167: 1–13.
21. Hadasik E., Pater Z., Obróbka plastyczna. Podstawy teoretyczne, Gliwice, Wydawnictwo Politechniki Śląskiej, 2013.